New variables in spherical geometry

David G. Dritschel

Mathematical Institute
University of St Andrews

http://www-vortex.mcs.st-and.ac.uk

Collaborators:
Ali Mohebalhojeh (Tehran $\rightarrow$ St Andrews)
Jemma Shipton & Robert Smith (St Andrews)

Vortex dynamics

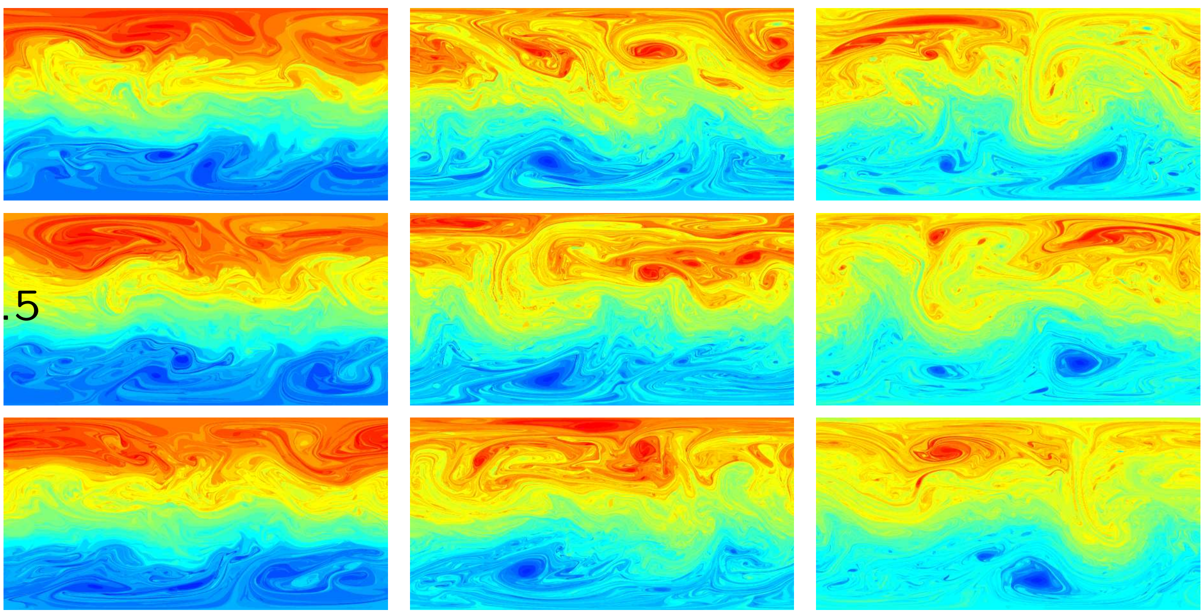

Froude number: $\mathrm{Fr} = \dfrac{|\boldsymbol{u}|}{c\sqrt{1+\tilde{h}}}$

Rossby number: $\mathrm{Ro} = \dfrac{\zeta}{2\Omega_E}$

$\dfrac{\varpi_{\mathrm{rms}}}{2\Omega_E} = \dfrac{1}{6}$ $\dfrac{\varpi_{\mathrm{rms}}}{2\Omega_E} = \dfrac{1}{3}$ $\dfrac{\varpi_{\mathrm{rms}}}{2\Omega_E} = \dfrac{1}{2}$

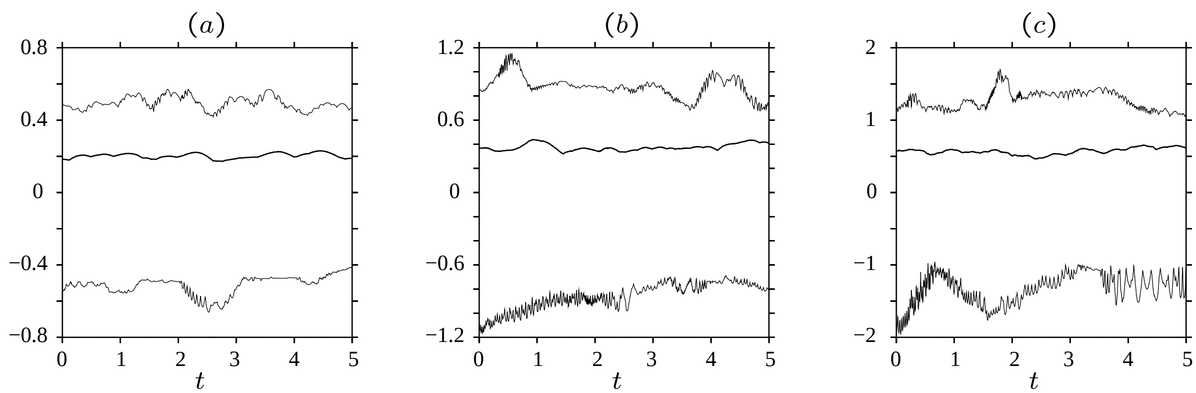

$\mathrm{Fr}_{\mathrm{max}}$: middle, **bold** curve

$\mathrm{Ro}_{\mathrm{max}}$: upper, thin curve

$\mathrm{Ro}_{\mathrm{min}}$: lower, thin curve

Depth anomaly, $\tilde{h}$

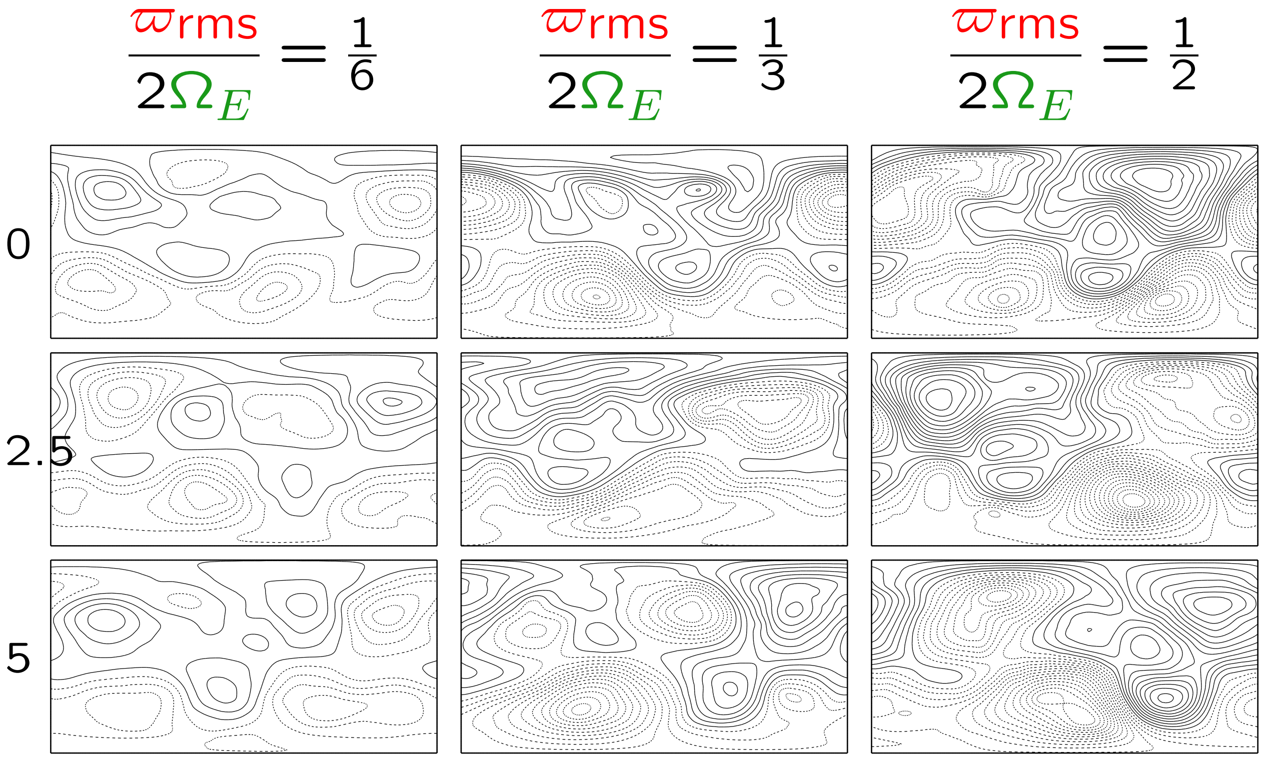

$$\Delta\tilde{h} = 0.02$$

Velocity divergence, $\delta/2\Omega_E$

$$\frac{\varpi_{\rm rms}}{2\Omega_E} = \frac{1}{6} \qquad \frac{\varpi_{\rm rms}}{2\Omega_E} = \frac{1}{3} \qquad \frac{\varpi_{\rm rms}}{2\Omega_E} = \frac{1}{2}$$

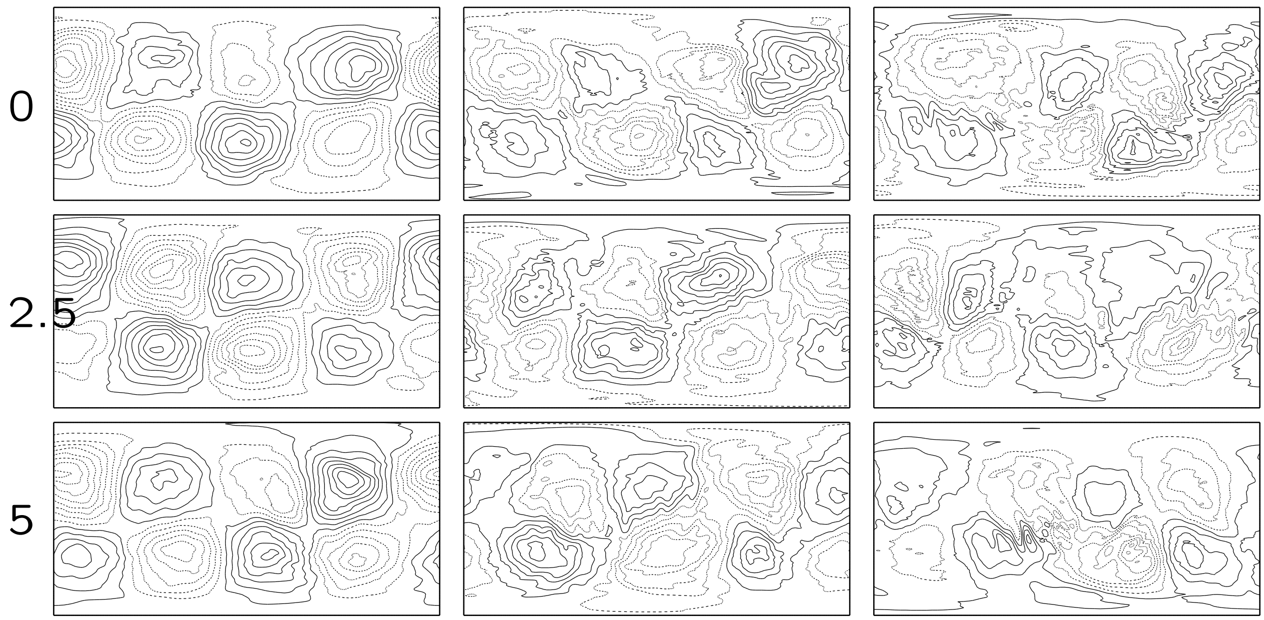

(0.002) (0.005) (0.010)

NB: In the time mean,

$$\frac{\delta_{\rm rms}}{\zeta_{\rm rms}} = 0.0373,\ 0.0466 \text{ and } 0.0653$$

Acceleration divergence, $\gamma/4\Omega_E^2$

$\frac{\varpi_{\rm rms}}{2\Omega_E} = \frac{1}{6}$ $\frac{\varpi_{\rm rms}}{2\Omega_E} = \frac{1}{3}$ $\frac{\varpi_{\rm rms}}{2\Omega_E} = \frac{1}{2}$

0

2.5

5

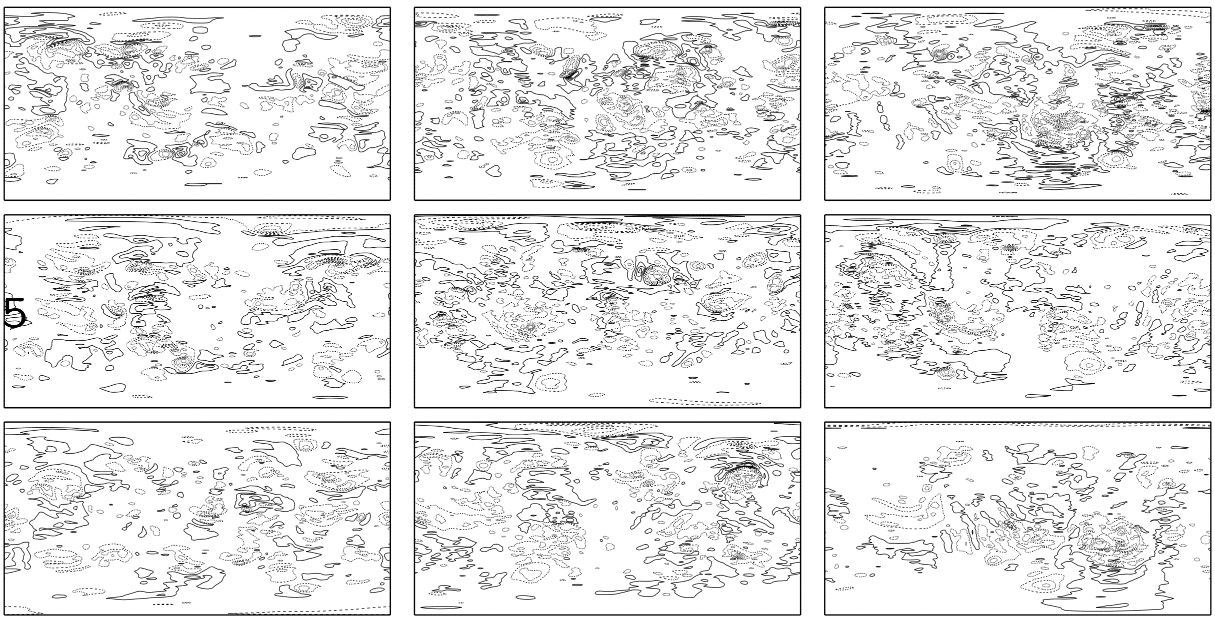

(0.02) (0.05) (0.10)

NB: In the time mean,

$$\frac{\gamma_{\rm rms}}{\zeta^2_{\rm rms}} = 0.767,\ 0.773 \text{ and } 0.847$$

Acceleration, $|\boldsymbol{a}|/4\Omega_E^2$

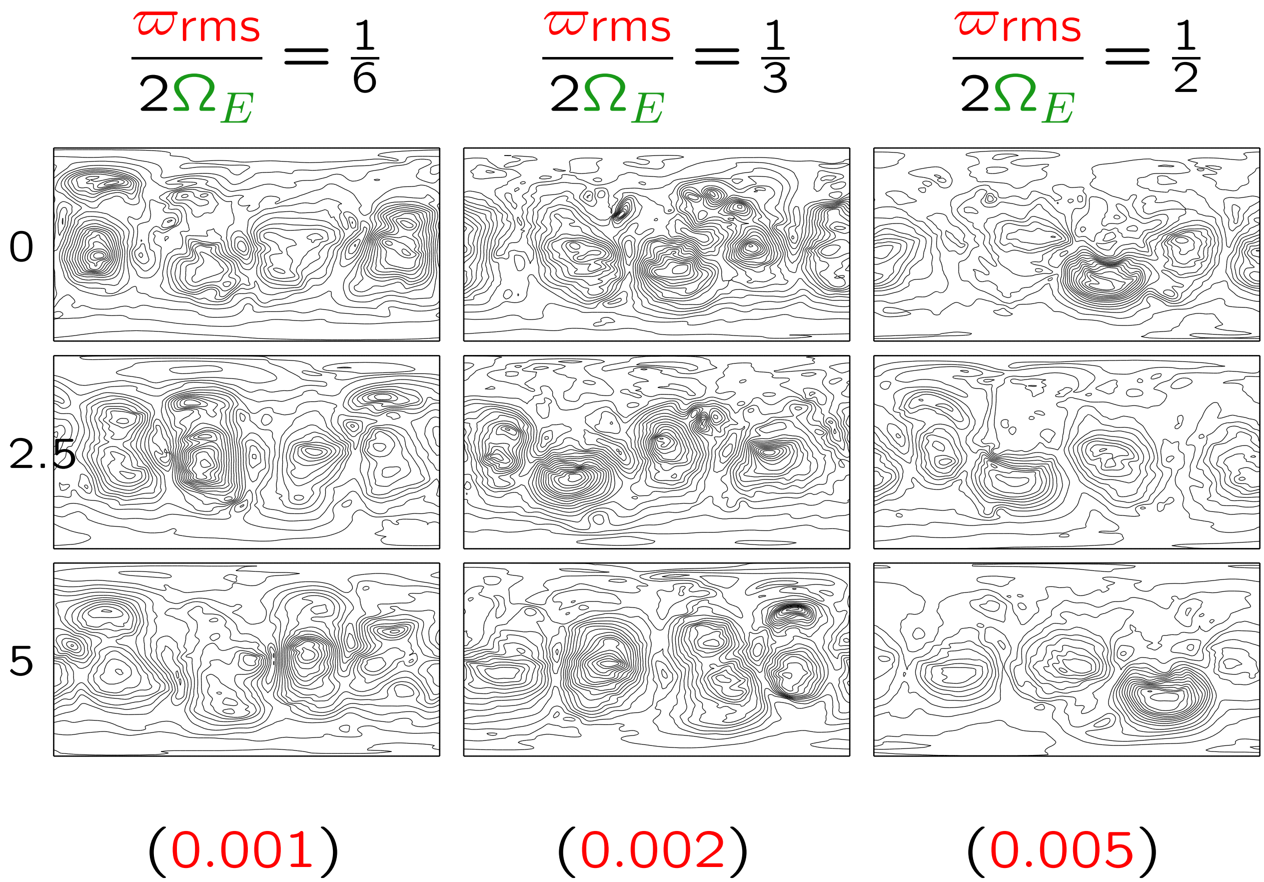

Meridional velocity, v, for the case $\frac{\varpi_{\mathrm{rms}}}{2\Omega_E} = \frac{1}{3}$

v_0: velocity obtained for $\delta = \gamma = 0$

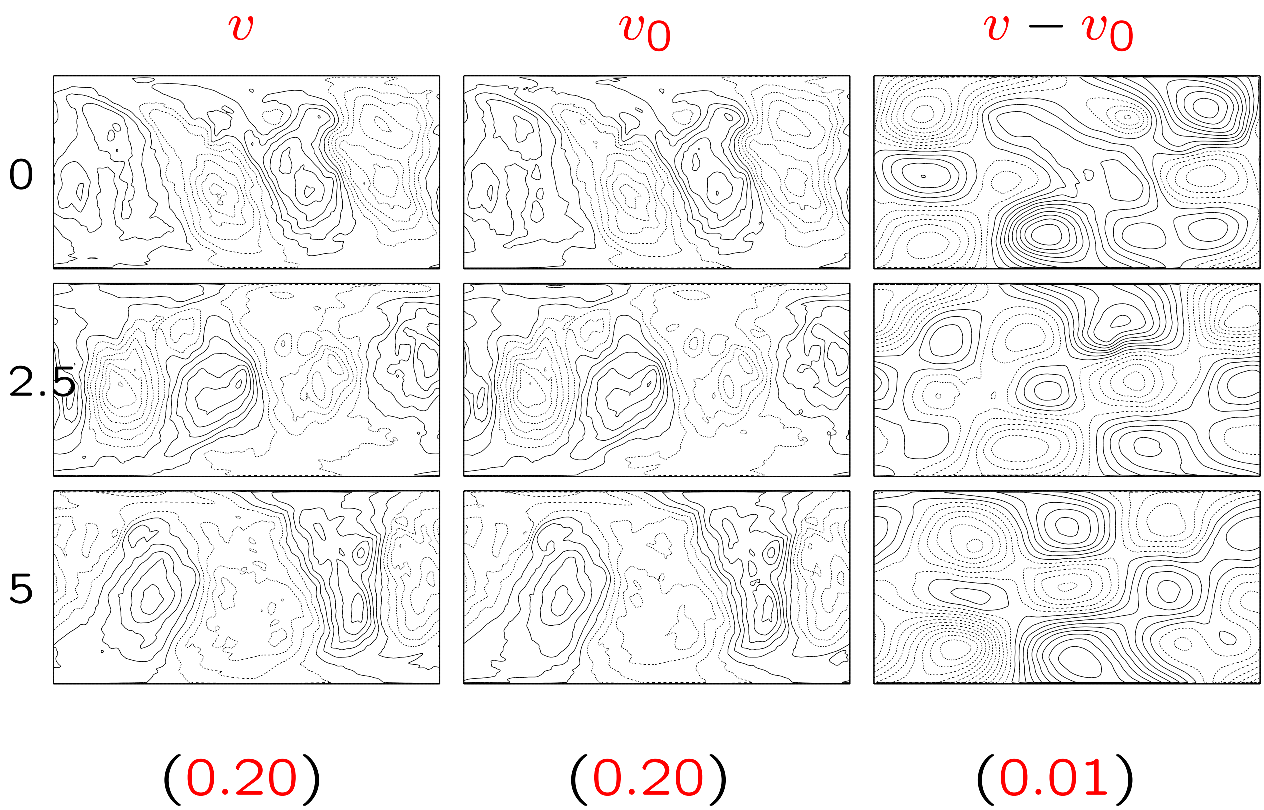

Why another shallow-water model?

• Explicit potential-vorticity (PV) conservation has never been implemented in spherical geometry.

• Wave–vortex decomposition not well understood even in this simple context.

• Accurate modelling of *both* the PV-controlled balanced flow and the imbalanced flow is now possible.

The shallow-water equations

$$\frac{\mathrm{D}\boldsymbol{u}}{\mathrm{D}t} + f\boldsymbol{k} \times \boldsymbol{u} = -c^2 \boldsymbol{\nabla} \tilde{h}$$

$$\frac{\partial \tilde{h}}{\partial t} + \boldsymbol{\nabla} \cdot [(1 + \tilde{h})\boldsymbol{u}] = 0$$

where $\tilde{h} \equiv (h - H)/H$, $c^2 = gH$, $f = 2\Omega_E \sin\phi$, H is the mean depth, g is gravity, and $\boldsymbol{u}$ is tangent to the sphere.

Dissipation and forcing terms are not included.

These equations may be combined to show

$$\frac{\mathrm{D}\Pi}{\mathrm{D}t} = 0, \quad \text{where} \quad \Pi = \frac{\zeta + f}{1 + \tilde{h}}$$

is the potential vorticity (PV).
NB: $\zeta = \boldsymbol{k} \cdot (\boldsymbol{\nabla} \times \boldsymbol{u})$.

New variables

The original equations hide PV conservation
$\Rightarrow$ numerically, PV is poorly conserved.

The distribution of PV largely controls the fluid motion $(\boldsymbol{u}, \tilde{h})$ through hidden balance relations (PV inversion).
— Hoskins, McIntyre & Robertson (1985), McIntyre & Norton (1999), Ford, McIntyre & Norton (2000), etc.

$\Rightarrow$ numerically, a poor representation of the PV leads to a poor representation of the fluid motion.

$\Rightarrow$ The residual motion, the "imbalance" (gravity waves), may be prone to **large** errors.

- Two distinct types of motion co-exist:
  - ◇ Slow "balanced" vortical motions, and
  - ◇ Relatively fast "imbalanced" wave motions

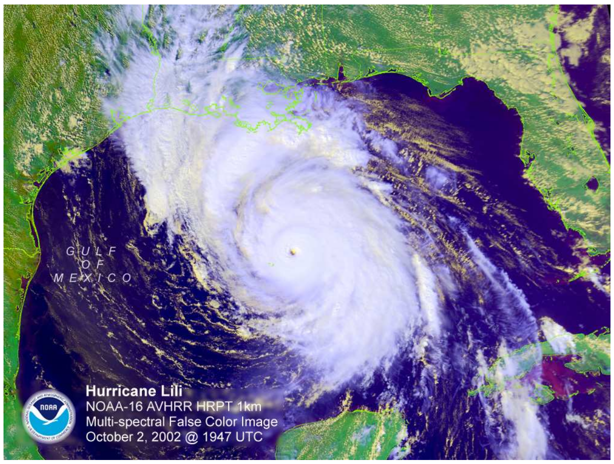

⇒ which however are deeply intertwined

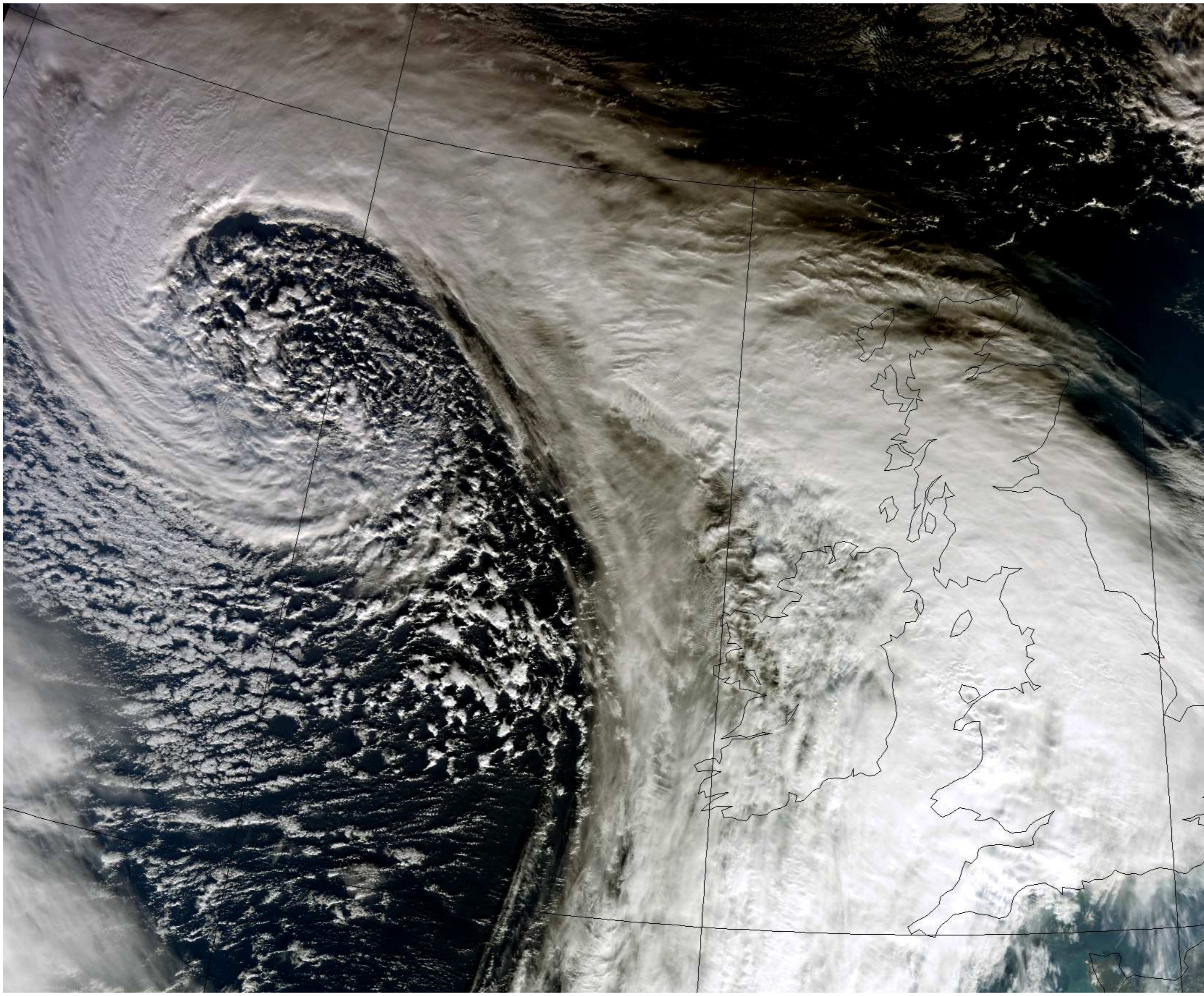

A new approach

- ◇ Enforce PV conservation explicitly
  (preserve its advective character)
  $\Rightarrow$ use *contour advection*;

- ◇ Distinguish the PV-controlled balanced motions and the residual imbalanced motions, at least to leading order
  $\Rightarrow$ use *imbalanced prognostic variables*.

— Dritschel & Mohebalhojeh (2000),
M & D (2000,2001,2004), D & Viúdez (2003),
V & D (2003,2004)

Explicit PV conservation

A particle representation for PV is natural:

each particle $\boldsymbol{x} = \boldsymbol{X}$ conserves its value of Π

$$\frac{\mathrm{D}\Pi}{\mathrm{D}t} = 0 \quad \Rightarrow \quad \frac{\mathrm{d}\boldsymbol{X}}{\mathrm{d}t} = \boldsymbol{u}(\boldsymbol{X}, t)$$

A contour representation is even more natural, since exchanging any pair of particles on a contour Π = constant does not alter the distribution of Π

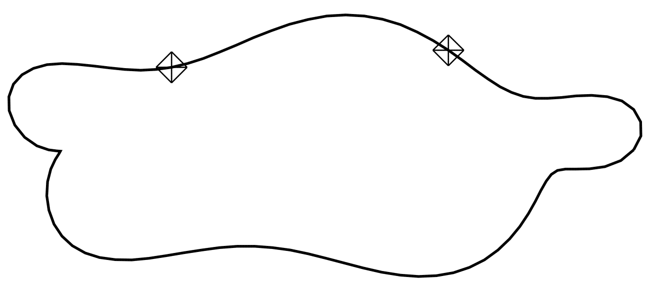

Numerics: an ideal algorithm?

The Contour-Advective Semi-Lagrangian (CASL) algorithm (Dritschel & Ambaum, 1997) makes direct use of this contour representation, *and* deals with the non-locality (inversion) efficiently.

It represents the PV by a finite set of contours

— the Lagrangian aspect —

represents the velocity by fixed grid points

— the Eulerian aspect —

and provides efficient means of communication between the two representations

— interpolation, and its inverse, filling.

Each PV contour is represented by *nodes*, connected together by cubic splines. Shown also is the underlying grid.

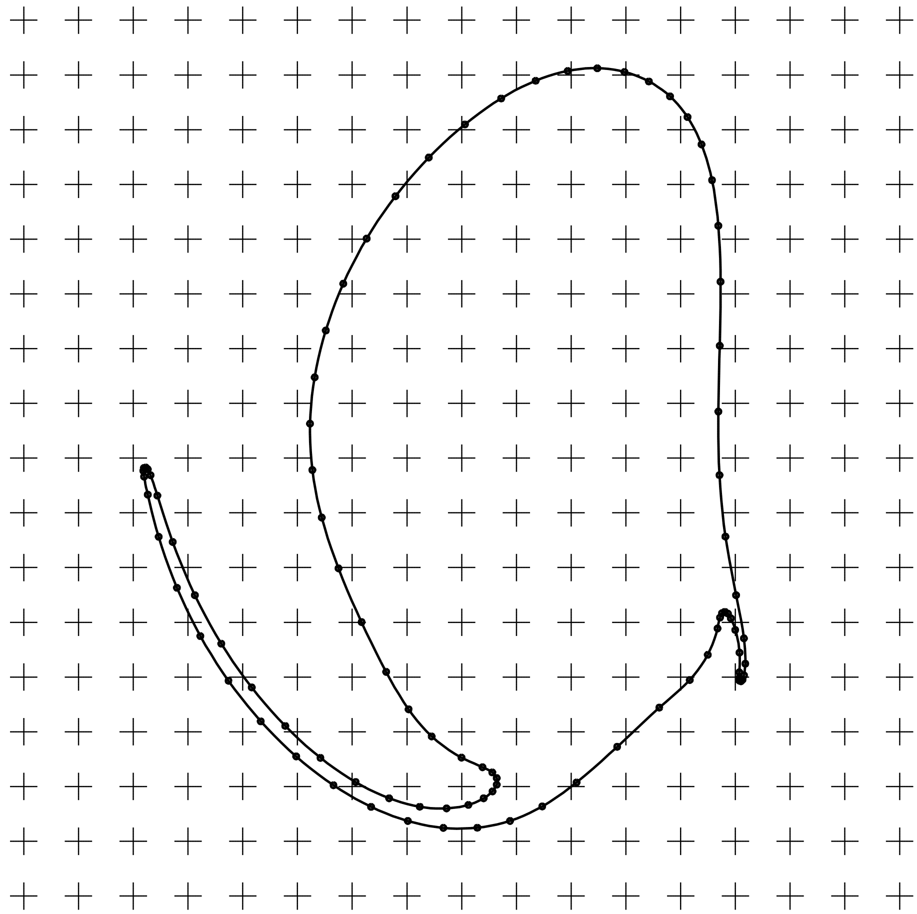

Note that Π is permitted to have much finer structure than $\boldsymbol{u}$. This exploits the fact that $\boldsymbol{u}$ is typically a *smoother* field than Π.

Balance relations

Having chosen the PV as one prognostic variable, what is a sensible (accurate *and* convenient) choice for the other two?

In a *balanced model*, the fluid motion $(\boldsymbol{u}_\mathsf{b}, \tilde{h}_\mathsf{b})$ is fully controlled by the PV. The balanced motion is recovered by PV inversion,
i.e. by solving equations of the form

$$\mathcal{F}(\boldsymbol{u}_\mathsf{b}, \tilde{h}_\mathsf{b}) = 0, \quad \mathcal{G}(\boldsymbol{u}_\mathsf{b}, \tilde{h}_\mathsf{b}) = 0, \quad \mathcal{H}(\boldsymbol{u}_\mathsf{b}, \tilde{h}_\mathsf{b}) = 0$$

for $\boldsymbol{u}_\mathsf{b}$ and $\tilde{h}_\mathsf{b}$, *given* the PV Π.

One of these equations comes from the definition of PV:

$$\mathcal{F} = \boldsymbol{k} \cdot (\boldsymbol{\nabla} \times \boldsymbol{u}_\mathsf{b}) + f - \Pi(1 + \tilde{h}_\mathsf{b}) = 0$$

The other two come from imposing particular relations between variables, e.g. as in geostrophic balance.

For example, one may set two successive time derivatives of the divergence $\delta = \boldsymbol{\nabla} \cdot \boldsymbol{u}$ to be zero, i.e.

$$\mathcal{G} = \delta^{(n)} = 0, \quad \mathcal{H} = \delta^{(n+1)} = 0$$

generating the "δ hierarchy". The forms of $\mathcal{G}$ and $\mathcal{H}$ are found by recursively substituting the original equations (M & D 2001).

Another example, used here, sets

$$\mathcal{G} = \delta^{(n)} = 0, \quad \mathcal{H} = \gamma^{(n)} = 0$$

where $\gamma = \boldsymbol{\nabla} \cdot \boldsymbol{a}$ and $\boldsymbol{a} = \mathrm{D}\boldsymbol{u}/\mathrm{D}t$.

NB: $\boldsymbol{a} = -f\boldsymbol{k} \times \boldsymbol{u} - c^2\boldsymbol{\nabla}\tilde{h}$

It makes sense that the new variables should represent what the PV cannot.

$\Rightarrow$ The new variables could be $\mathcal{G}$ and $\mathcal{H}$ themselves.

Here, we use the simplest member, $n = 0$, of the δ-γ hierarchy. In other words, we take

$$\mathcal{G} = \delta, \qquad \mathcal{H} = \gamma$$

to be the other two prognostic variables.

On the f-plane, γ is proportional the "ageostrophic vorticity", $\zeta - c^2\nabla^2\tilde{h}/f$.

Setting $\gamma = \delta = 0$ then leads to geostrophic balance (cf. M & D 2001). The variables γ and δ thus represent the *departure* from geostrophic balance.

On the sphere,

$$\gamma = f\zeta - \beta u - c^2\nabla^2\tilde{h}$$

where $\beta = \mathrm{d}f/\mathrm{d}\phi = 2\Omega_E\cos\phi$
and u is the zonal velocity component.

The prognostic equations for δ and γ are

$$\frac{\partial \delta}{\partial t} = \gamma - |\boldsymbol{u}|^2 - 2\left[\frac{\partial u}{\partial \phi}\left(\frac{\partial u}{\partial \phi} + \zeta\right) + \frac{\partial v}{\partial \phi}\left(\frac{\partial v}{\partial \phi} - \delta\right)\right] - \boldsymbol{\nabla}\cdot(\delta \boldsymbol{u})$$

$$\frac{\partial \gamma}{\partial t} = c^2 \nabla^2 \{\boldsymbol{\nabla}\cdot[(1+\tilde{h})\boldsymbol{u}]\} + 2\Omega_E \frac{\partial B}{\partial \lambda} - \boldsymbol{\nabla}\cdot(Z\boldsymbol{u})$$

where $B \equiv c^2\tilde{h} - \frac{1}{2}|\boldsymbol{u}|^2$ (Bernoulli pressure), $Z = f(\zeta + f)$, and λ is longitude.

However, the tendencies involve the original variables $\boldsymbol{u}$ and $\tilde{h}$. These are recovered by a kind of PV inversion analogous to what is done in a balanced model.

Inversion

Inversion here simply means finding $\boldsymbol{u}$ and $\tilde{h}$ from the prognostic variable set (δ, γ, Π).

This is accomplished as follows. Let

$$\boldsymbol{u} = \boldsymbol{k} \times \boldsymbol{\nabla}\psi + \boldsymbol{\nabla}\chi$$

then the potentials satisfy

$$\nabla^2\psi = \zeta \quad \& \quad \nabla^2\chi = \delta\,.$$

But ζ depends on $\tilde{h}$ through the definition of PV:

$$\zeta = (1 + \tilde{h})\Pi - f\,.$$

So, we need to find $\tilde{h}$ before we can invert ζ. But the definition of γ implies

$$c^2\nabla^2\tilde{h} - f\Pi\tilde{h} = f(\Pi - f) - \beta u - \gamma\,,$$

using ζ above.

While the inversion equations are coupled, they are *linear*, an exceptional property.

Numerically, they are solved iteratively and convergence is exponentially fast.

Solve $\nabla^2 \chi = \delta$ first $\Rightarrow \boldsymbol{u}_\chi$.

Then iteratively solve

$$\nabla^2 \psi_{n+1} = \zeta_n = (1 + \tilde{h}_n)\Pi - f \;\Rightarrow \boldsymbol{u}_{n+1}$$

and

$$(c^2 \nabla^2 - f^2)\tilde{h}_{n+1} = f(\zeta_n - f\tilde{h}_n) - \beta u_{n+1} - \gamma$$

$\Rightarrow \psi_{n+1}$ and $\tilde{h}_{n+1}$.

Numerics

◇ All fields represented on a regular lat-lon grid, with $\Delta\phi = \Delta\lambda/2 \quad (n_\phi = n_\lambda)$

◇ Semi-spectral approach: advantageous for inverting $c^2\nabla^2 - f^2$ (tridiagonal procedure)

◇ 2nd-order finite differences in ϕ

◇ Semi-implicit time stepping, but

$$\Delta t < \Delta t_{\text{CFL}} = \Delta\phi/c$$

◇ Minimal Robert-Asselin filtering: $A = c\Delta t$

◇ 2/3 spectral filter applied to nonlinear parts of δ & γ tendencies:

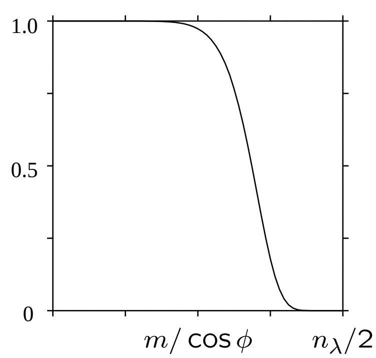

(D & V 2003)

Verification

◇ Standard Rossby-Haurwitz wave test and a perturbed variation (cf. Thuburn & Li 2000)

$t = 0$ $\quad$ $t = 5$

Π (0.6)

$\tilde{h}$ (0.02)

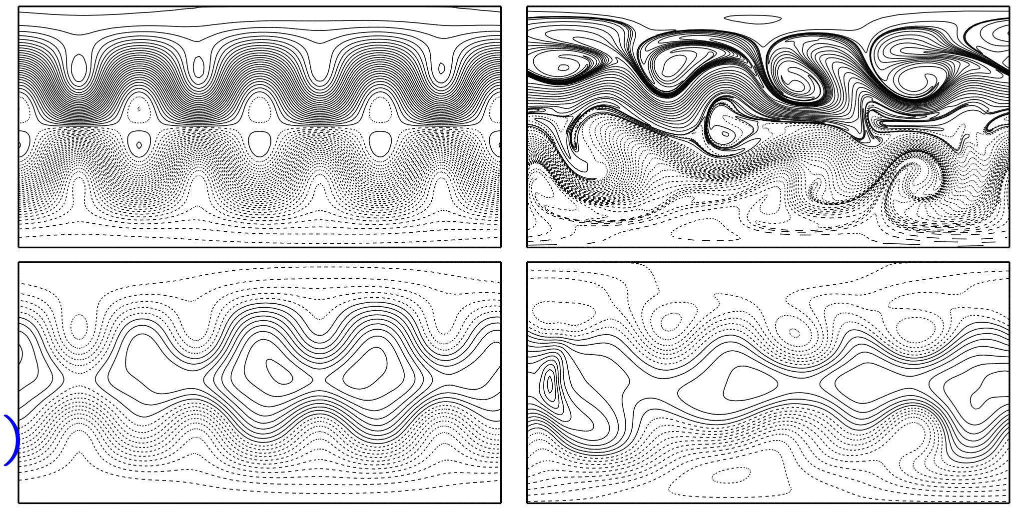

$\Rightarrow$ 0.22% energy variation over 5 days

$\Rightarrow$ 0.31% angular momentum variation

$$\textit{Note}: \quad n_\phi = n_\lambda = 128$$

◇ Usual spatial and temporal resolution variations

An application to turbulence

◇ Random PV anomaly $\varpi = \Pi - f$ spatially correlated over a length $L_c = 1/10$

ϖ, polar view $\qquad$ ϖ, equatorial view

◇ Prescribed mean Rossby radius

$$L_R = c/2\Omega_E = 1/3$$

◇ Planetary rotation $\Omega_E = 2\pi$

◇ $n_\phi = n_\lambda = 128$, $\Delta t = 0.004$ $(\Delta t_{\text{CFL}} = 0.0058)$

Initialisation (V & D 2003, D & V 2003)

Generate initial fields of δ and γ ($\Rightarrow \boldsymbol{u}$ and $\tilde{h}$) by *ramping up* the PV anomaly ϖ from 0 to its desired amplitude over a period $\Delta\tau_I \gg 1$:

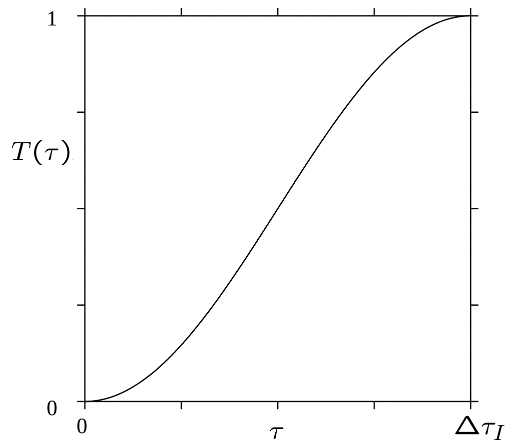

Meanwhile, evolve δ and γ using the *full* model, **and** advect the PV contours.

$$\delta = \gamma = \boldsymbol{u} = \tilde{h} = 0 \quad \text{at} \quad \tau = 0.$$

NB: the PV jump across each contour increases like $T(\tau)$.

The state at $\tau = \Delta\tau_I$ is considered the initial state, $t = 0$.

PV contours at $\tau = 0$ | PV contours at $\tau = \Delta\tau_I$

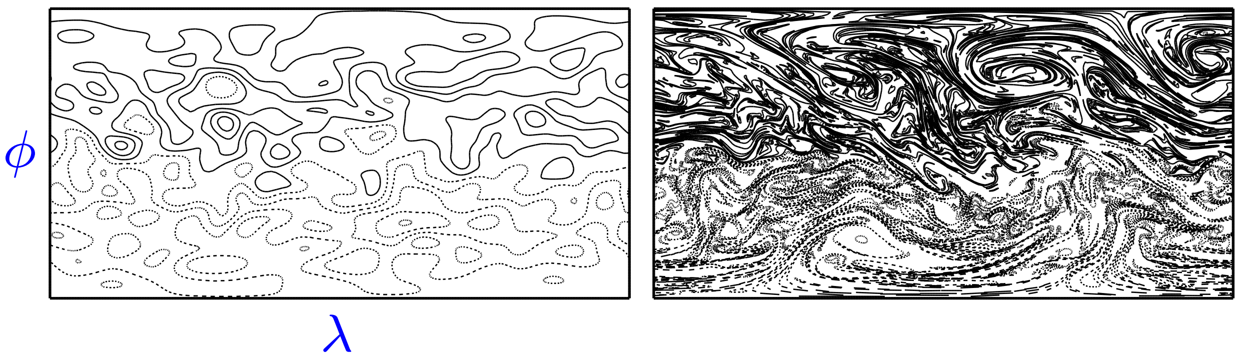

Note, $\Pi = f$ on the left since $T(0) = 0$.

◇ Here $\Delta\tau_I = 20$ days in <u>three</u> cases:

$$\frac{\varpi_{\text{rms}}}{2\Omega_E} = \frac{1}{6}, \quad \frac{1}{3}, \quad \text{and} \quad \frac{1}{2}.$$

Gravity waves

It is common to call the residual imbalance "gravity waves", but this can be misleading. The balanced flow can be defined in **many** ways.

We could make use of the balance hierarchies such as $\delta^{(n)} = \gamma^{(n)} = 0$, but they prove ineffective for highly nonlinear flows.

A new alternative, called the Optimal PV (OPV) balance (V & D 2004), is to define the *PV-controlled* balanced flow as

> the flow which "evolves" into the current PV distribution after a *long* ramp period $\Delta\tau_D$

That is, we seek the *base configuration* $\boldsymbol{X}_{\text{base}}$ of PV contours, at a time $t - \Delta\tau_D$, which evolves <u>into</u> the current PV contours $\boldsymbol{X}$ while ramping up the PV as in initialisation — *from a state of no motion*.

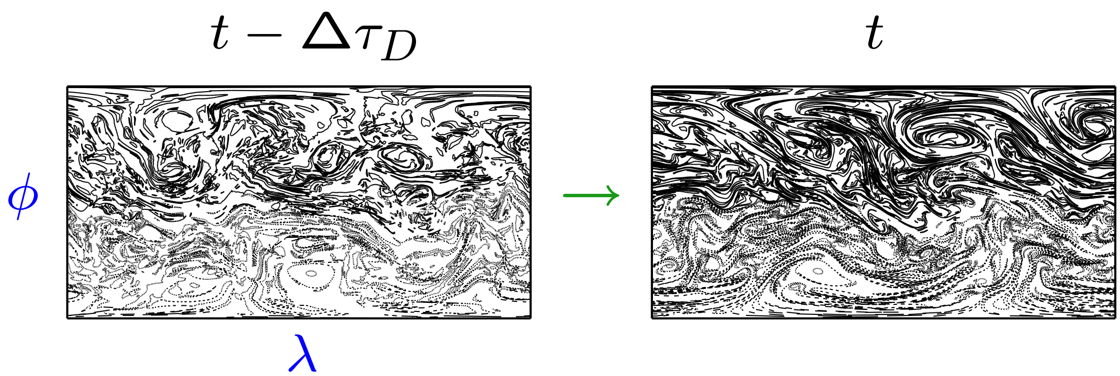

The fields of $\tilde{h}$, δ, γ, etc. at the end of this ramped evolution are called the balanced fields, $\tilde{h}_{\mathsf{b}}$, δ_{b}, γ_{b}, etc.

In practice, $\boldsymbol{X}_{\mathsf{base}}$ and hence $\tilde{h}_{\mathsf{b}}$, δ_{b}, γ_{b}, etc. are found *iteratively* in a cycle of forward and backward integrations (V & D 2004).

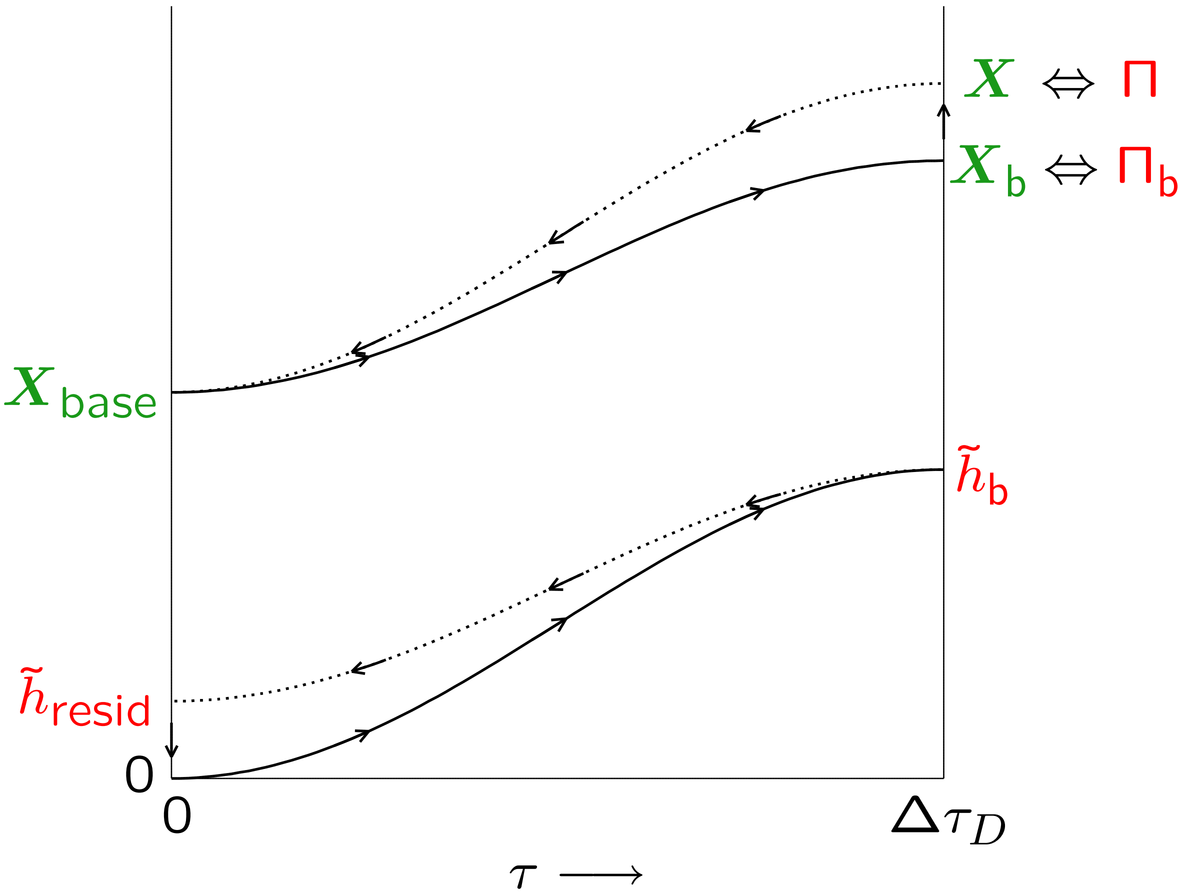

$\tilde{h}_{\mathsf{b}}$, δ_{b}, γ_{b}, etc. depend *only* on Π and $\Delta\tau_D$.

The imbalanced fields are $\tilde{h}_{\mathsf{i}} \equiv \tilde{h} - \tilde{h}_{\mathsf{b}}$, $\delta_{\mathsf{i}} \equiv \delta - \delta_{\mathsf{b}}$, $\gamma_{\mathsf{i}} \equiv \gamma - \gamma_{\mathsf{b}}$, etc.

Convergence

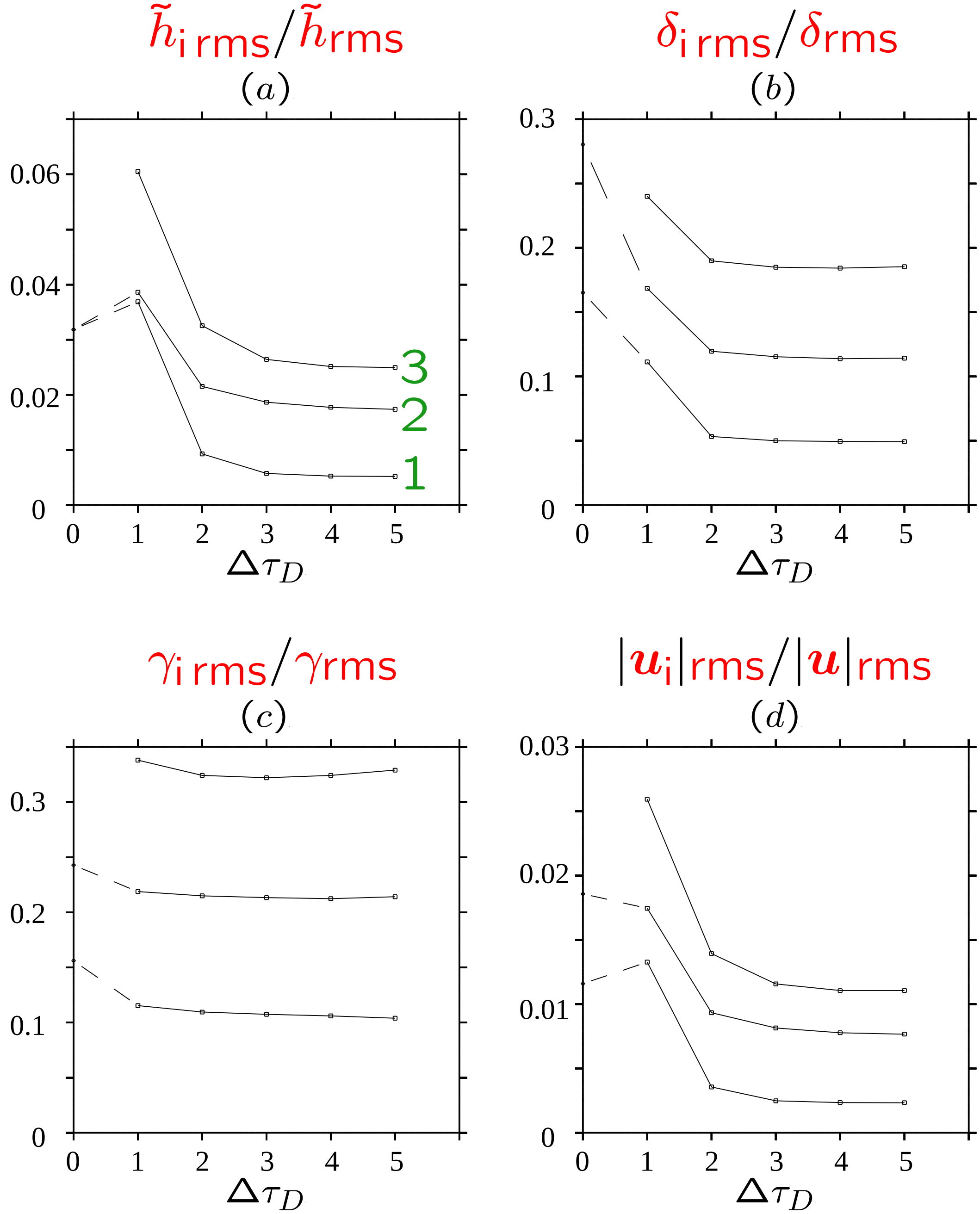

1^{st}-order δ–γ balance is plotted along $\Delta\tau_D = 0$.

Comparison

Balance	$\dfrac{\tilde{h}_{\mathrm{i\,rms}}}{\tilde{h}_{\mathrm{rms}}}$	$\dfrac{\delta_{\mathrm{i\,rms}}}{\delta_{\mathrm{rms}}}$	$\dfrac{\gamma_{\mathrm{i\,rms}}}{\gamma_{\mathrm{rms}}}$	$\dfrac{\lvert\boldsymbol{u}_{\mathrm{i}}\rvert_{\mathrm{rms}}}{\lvert\boldsymbol{u}\rvert_{\mathrm{rms}}}$
$\delta = \gamma = 0$	0.1418	1.000	1.000	0.0740
$\dfrac{\partial\delta}{\partial t} = \dfrac{\partial\gamma}{\partial t} = 0$	0.0318	0.280	0.243	0.0186
OPV, $\Delta\tau_D = 5$	0.0174	0.114	0.214	0.0077

All results are for $\dfrac{\varpi_{\mathrm{rms}}}{2\Omega_E} = \frac{1}{3}$

Imbalanced depth $\tilde{h}_{\text{i}}$ at $t = 5$ for $\frac{\varpi_{\text{rms}}}{2\Omega_E} = \frac{1}{3}$

$\delta = \gamma = 0$

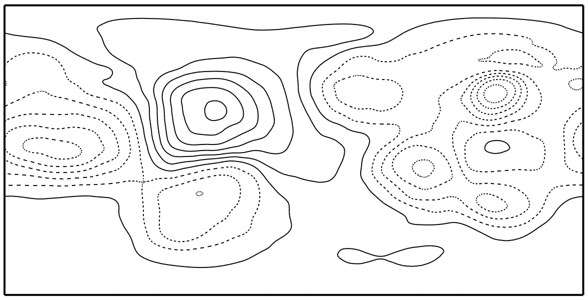

$\frac{\partial \delta}{\partial t} = \frac{\partial \gamma}{\partial t} = 0$

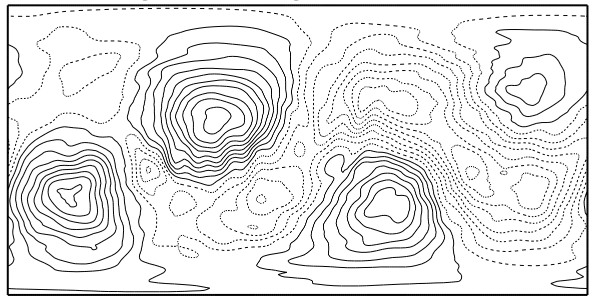

OPV, $\Delta\tau_D = 2$

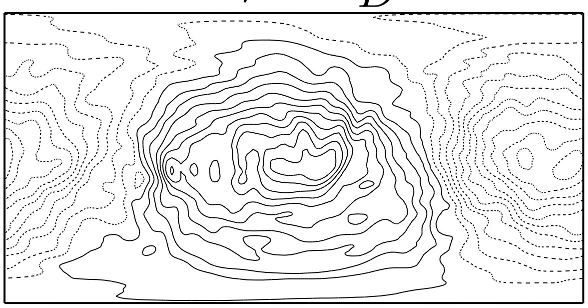

OPV, $\Delta\tau_D = 3$

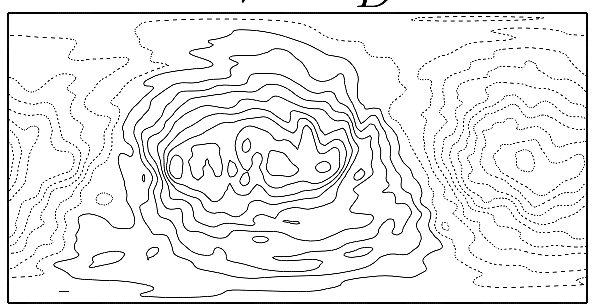

OPV, $\Delta\tau_D = 4$

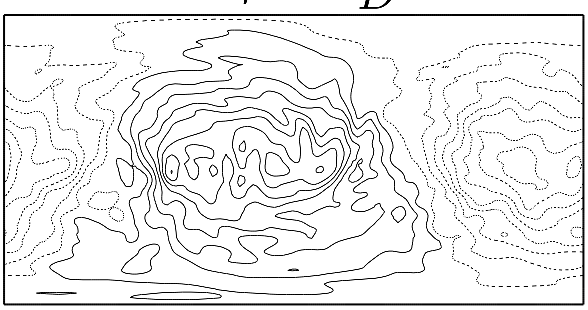

OPV, $\Delta\tau_D = 5$

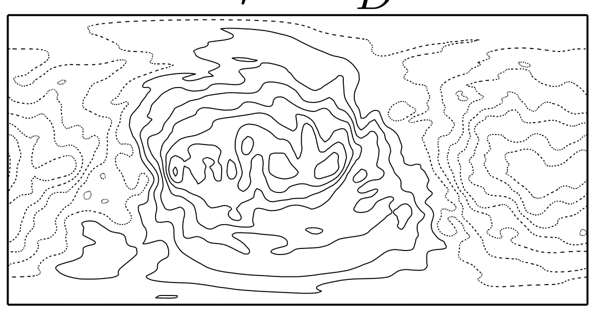

$\Delta\tilde{h} = 0.0005$ except for $\delta = \gamma = 0$ balance for which $\Delta\tilde{h} = 0.005$.

Velocity divergence $\delta/2\Omega_E$ at $t = 5$

$\frac{\varpi_{\text{rms}}}{2\Omega_E} = \frac{1}{6}$ $\frac{\varpi_{\text{rms}}}{2\Omega_E} = \frac{1}{3}$ $\frac{\varpi_{\text{rms}}}{2\Omega_E} = \frac{1}{2}$

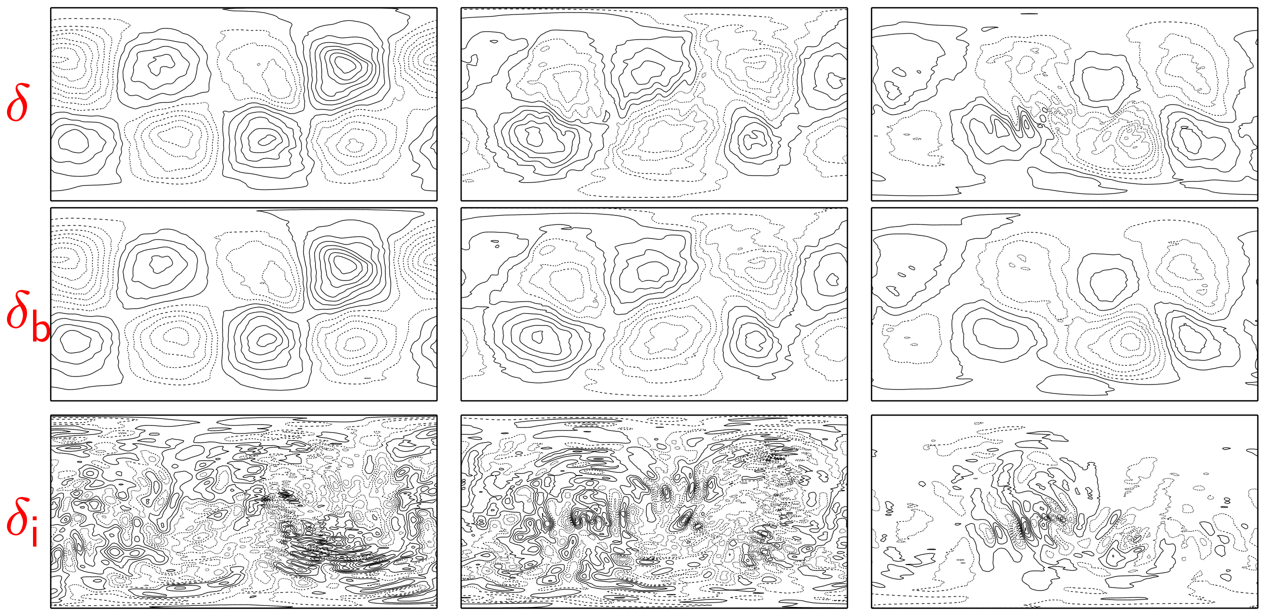

(0.002, 0.0002) (0.005, 0.001) (0.010, 0.005)

NB: All results are henceforth for $\Delta\tau_D = 5$

Imbalanced depth anomaly, $\tilde{h}_{\mathrm{i}}$

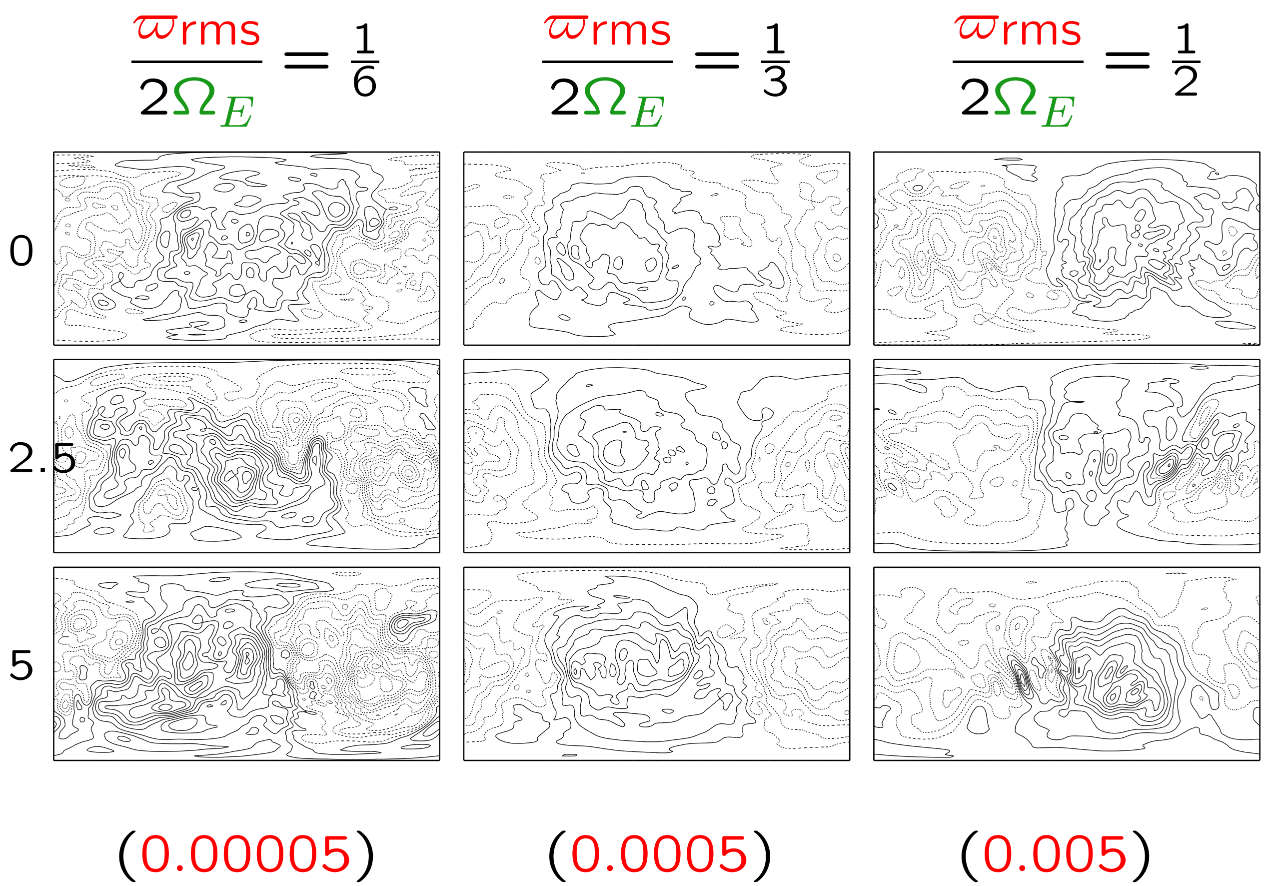

Imbalanced velocity divergence, $\delta_{\mathrm{i}}/2\Omega_E$

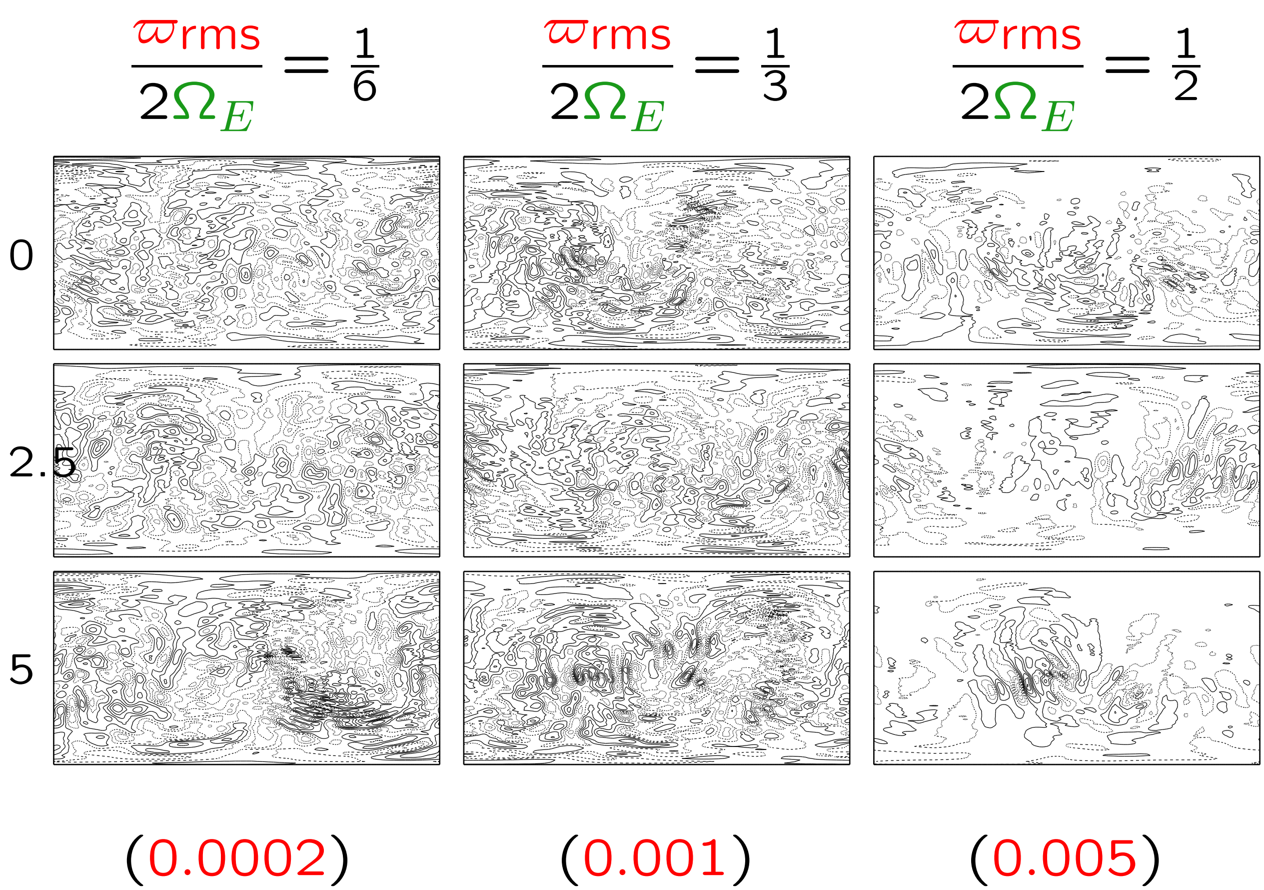

Imbalanced acceleration divergence, $\gamma_{\mathrm{i}}/4\Omega_E^2$

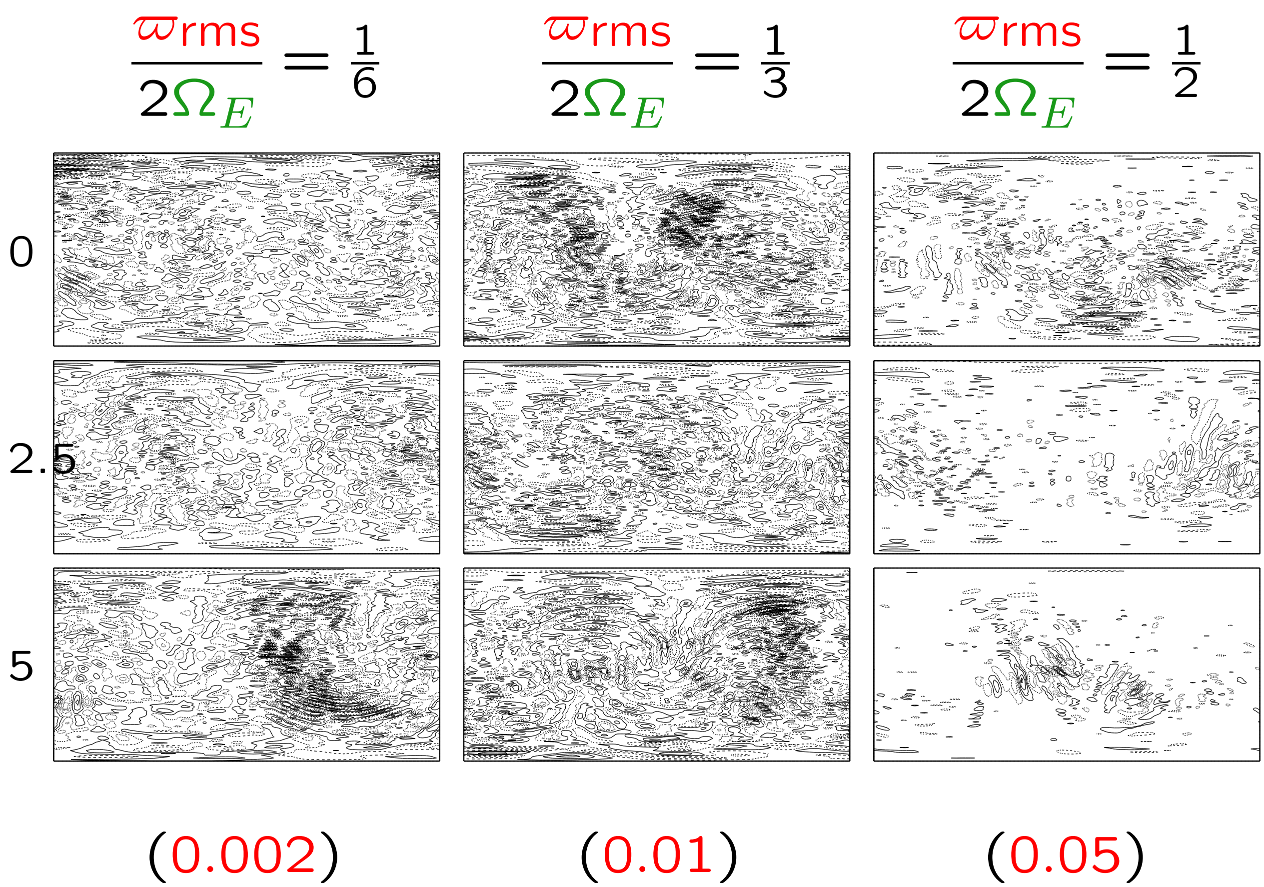

Frequency spectra

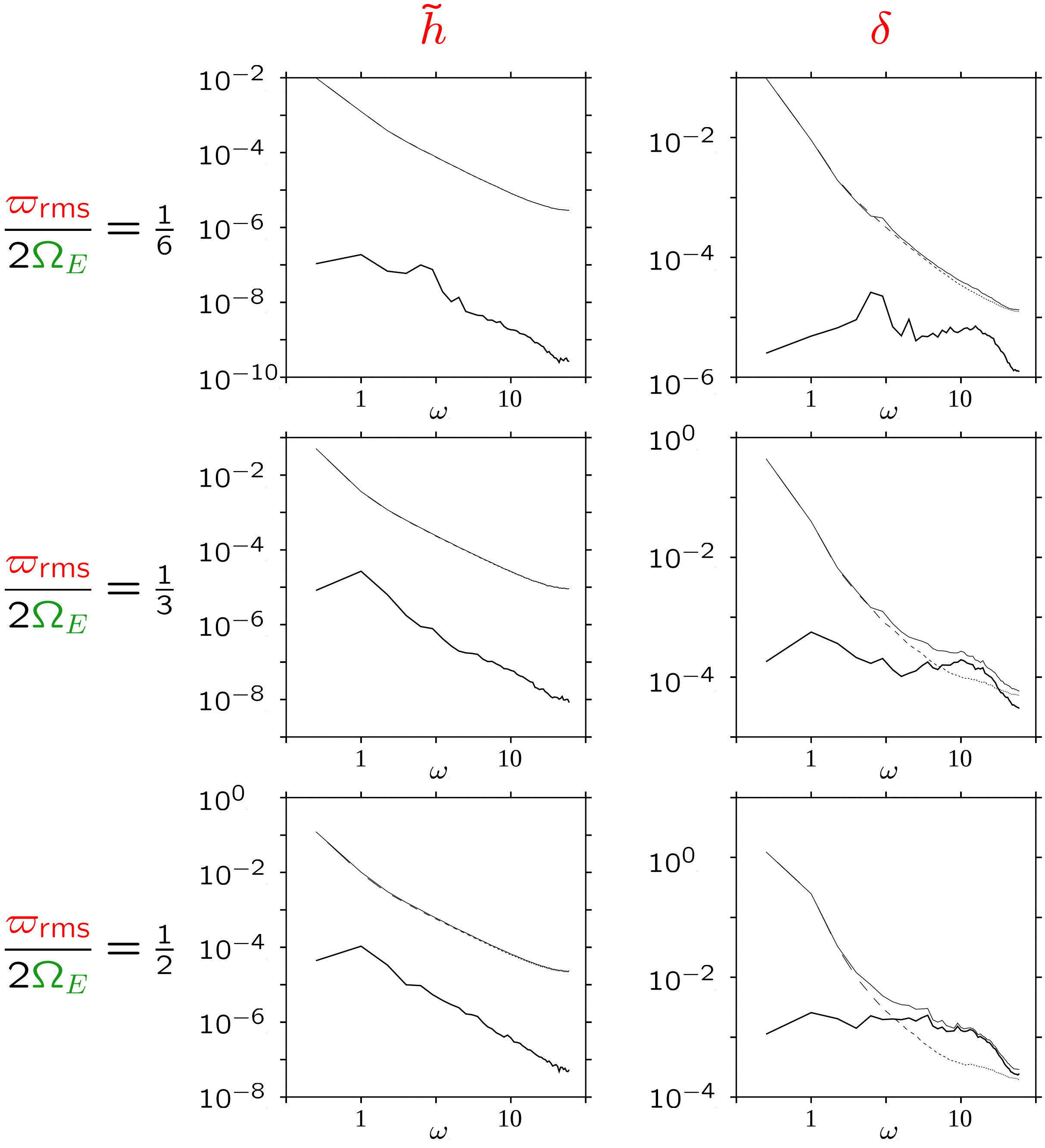

Finalé

- Greater accuracy can be achieved by *explicitly* distinguishing the vortical and the wave components of a flow.

- Gravity waves are more clearly identified when taking full account of the flow inertia, as in the OPV balance procedure.

- Similar results have been found for both spherical shallow-water flows and for three-dimensional non-hydrostatic flows.